

# The Partitioning of PAHs to Egg Phospholipids Facilitated by Copper and Proton Binding via Cation- $\pi$ Interactions

XIAOLEI QU, XIAORONG WANG, AND DONGQIANG ZHU\*

State Key Laboratory of Pollution Control and Resource Reuse, and School of the Environment, Nanjing University, Jiangsu 210093, P.R. China

Received July 21, 2007. Revised manuscript received September 24, 2007. Accepted September 25, 2007.

The partitioning to lipid-containing solids (cell membranes, natural organic matters) plays an important role in the fate of organic pollutants. We herein studied sorption of a series of aromatic compounds from aqueous solution to gel-phase egg phospholipids. The regression line describing the free-energy relationship between lipid–water distribution coefficient ( $K_d$ ) and *n*-octanol–water partition coefficient ( $K_{OW}$ ) for the high-polar compounds (phenolics, dinitrobenzene, trinitrobenzene) is displaced upward relative to the low-polar compounds (chlorobenzenes, polycyclic aromatic hydrocarbons (PAHs), nitrobenzene, dichlorobenzonitrile), suggesting additive polar extra-interactions besides hydrophobic effects in sorption. Binding of  $\text{Cu}^{2+}$  or decreasing pH increases sorption of the three and four-ring PAHs but not the rest compounds. These results led us to propose a specific sorption mechanism, cation- $\pi$  bonding between PAHs and complexed metal ions or protonated amine groups of phospholipids. The  $\text{Cu}^{2+}$ -PAH complexation in solution was supported by the observation that PAHs enhance the saturated solubility of  $\text{CuSO}_4$  in chloroform, and the enhancement correlates with  $\pi$ -donor strength of PAH (pyrene > phenanthrene > naphthalene). The electron coupling between the protonated amine groups of phospholipids and PAHs in chloroform was verified by the electronic deshielding-induced downfield chemical shifts of phenanthrene at low pH in the  $^1\text{H}$  NMR spectrum.

## Introduction

Biogenic lipids, including phospholipids, lipoproteins, fats, and sterols, are a group of biosynthetic chemicals that are widely distributed in the biosphere. To organisms the partitioning to biolipids is a key process that controls the exposure, retention, and biological reactivity of organic pollutants. One prominent example is that adipose tissues of high-trophic mammals tend to accumulate recalcitrant, lipophilic organic pollutants such as polycyclic aromatic hydrocarbons (PAHs) along the food chain, finally becoming the sink of these chemicals (1).

An important category of biolipids are phospholipids that form the bilayer structure of cell membranes, wherein the hydrophobic groups are directed inward and the hydrophilic groups are directed to the exterior of the membrane. As the

cytoplasmic membrane controls the transport of molecules into the cell, elucidation of the fundamental mechanisms that determine the organic–phospholipid bilayer interactions is of great theoretical and practical importance. For example, in drug design, the partitioning of drugs to the phospholipid liposome as chromatographic stationary phase, vesicle, gel phase, or homogeneous solution has often been used as a model for investigating drug–membrane interactions (2–7). In these studies, for nonionic chemicals a good linear free-energy relationship generally exists between lipid–water distribution coefficient ( $K_d$ ) and chemical *n*-octanol–water partition coefficient ( $K_{OW}$ ), indicating the hydrophobic partition mechanism. Furthermore, preferential partition of organic pollutants into the hydrophobic regions of phospholipid bilayer may impair vital functions of the cytoplasmic membrane, therefore causing toxic effects to the cell. Not surprisingly, a good correlation is often found between the toxicity of a given organic chemical and its  $K_{OW}$  value (8).

The environmental importance of biolipids is also reflected by the impact of soil lipids on sorption of organic pollutants by soil organic matter (SOM) (9, 10), as well as on the physical and biological properties of soil (11). Soil lipids are operationally defined as water-insoluble but organic solvent-extractable organic matters in the SOM matrix, composing a mixture of fatty acids, sterols, long-chain hydrocarbons, fats, waxes, etc. generated from exudation and decomposition of fauna, flora, and microorganisms (11, 12). Previous studies showed that despite the relative low content (i.e., between 4 and 8%, ref 13) in SOM, lipids naturally present in soil compete with organic solutes effectively for high affinity sorption sites of SOM, and removal of the lipid content greatly increases their sorptive nonlinearity and capacity (9, 10).

As common toxicants or micronutrients, heavy metals such as copper and lead often coexist with organic pollutants at contaminated sites. For example, many polluted soils contain PAHs, organic solvents, pesticides, and heavy metals in addition to all naturally occurring chemical species (e.g., alkali and alkaline earth metals, trace metals, anions) (14, 15). Biolipids can be a favorable phase for partitioning hydrophobic organic pollutants, and in the mean time for binding heavy metal ions via chemical coordination to the O-, P-, and N-containing functional groups. Binding of heavy metal ions to biopolymers, including phospholipids, is expected to influence the sorption of organic pollutants by modifying the structure and chemistry of the biopolymer, therefore impacting the environmental fate of organic pollutants. Xiao et al. (16) recently reported that presence of transition metals ( $\text{Ag}^+$ ,  $\text{Cu}^{2+}$ ,  $\text{Fe}^{3+}$ ) increases sorption of phenanthrene and tetrachlorobenzene by several times to the bacterial cell wall (structured with polysaccharide, cross-linked short peptides, lipoproteins, organic acids). The investigators suggested that metal complexation neutralizes the negative charge of the bacterial surface, making it less hydrophilic and enhancing hydrophobic partition of the organic solute. Furthermore, the mechanism of electron-coupling between PAHs (electron-donors) and complexed transition metal ions (electron-acceptors) on the bacterial surface was explored to explain the stronger facilitated sorption of PAHs by metals compared to chlorobenzenes considered non- $\pi$ -donors. Characterizing the cosorption of organic pollutants and heavy metal ions to phospholipids, which form the bilayer structure of cell membranes, may also shed light on understanding mechanisms of cototoxicity to cells exposed to metal–organic combined pollutions.

\* Corresponding author phone (fax): 86 025-8359-6496; e-mail: zhud@nju.edu.cn.

**TABLE 1. Sorbate *n*-Octanol–Water Partition Coefficient ( $K_{OW}$ ), Phospholipid–Water Distribution Coefficient with and without Presence of  $Cu^{2+}$  (Corresponding to  $K_{d,Cu}$  and  $K_d$ ), and the Ratio of  $K_{d,Cu}$  to  $K_d$** 

compound	abbrev.	$K_{OW}^a$ (L L <sup>-1</sup> )	$K_d^b$ (L kg <sup>-1</sup> )	$K_{d,Cu}^b$ (L kg <sup>-1</sup> )	$K_{d,Cu}/K_d$
naphthalene	NAPH	2140	2410 ± 40	2400 ± 100	1.0
phenanthrene	PHEN	37200	28000 ± 2000	48000 ± 4000	1.7
anthracene	ANEN	47900	42000 ± 9000	220000 ± 20000	5.2
pyrene	PYR	135000	72000 ± 6000	180000 ± 30000	2.5
1,2-dichlorobenzene	DCB	2510	2140 ± 80	2090 ± 70	0.98
1,2,4,5-tetrachlorobenzene	TeCB	52500	17000 ± 1000	16300 ± 900	0.96
nitrobenzene	NBZ	70.8	82 ± 7	92 ± 7	1.1
1,3-dinitrobenzene	DNB	1.49	100 ± 10	90 ± 7	0.90
1,3,5-trinitrobenzene	TNB	15.2	90 ± 8	70 ± 20	0.78
phenol	PHOL	27.5	72 ± 4	68 ± 3	0.94
2,4-dichlorophenol	DCP	1230	8500 ± 400	8700 ± 500	1.0
2,6-dichlorobenzonitrile	DNL	550 <sup>c</sup>	470 ± 20	500 ± 10	1.1

<sup>a</sup> From Schwarzenbach et al. (38) except where noted. <sup>b</sup> Average values on all sorption points (with ± standard deviations). <sup>c</sup> Calculated by ChemOffice 2005.

In this study, we systematically examined effects of copper and proton binding on sorption of organic compounds with varied physical–chemical properties (hydrophobicity, electron polarizability, polarity) to gel-phase egg phospholipids for better knowledge of organic–phospholipid interactions.

## Experimental Section

**Materials.** Sorbates include four PAHs, naphthalene (NAPH, Aldrich), phenanthrene (PHEN, Fluka), anthracene (ANEN, Fluka) and pyrene (PYR, Aldrich), two chlorobenzenes, 1,2-dichlorobenzene (DCB, Aldrich) and 1,2,4,5-tetrachlorobenzene (TeCB, Aldrich), two phenolics, phenol (PHOL, Aldrich) and 2,4-dichlorophenol (DCP, Aldrich), and three nitroaromatic compounds (NACs), nitrobenzene (NBZ, Aldrich), 1,3-dinitrobenzene (DNB, Aldrich) and 1,3,5-trinitrobenzene (1000 mg/L in acetonitrile) (TNB, Supelco), and 2,6-dichlorobenzonitrile (DNL, Chem Service). Sorbate  $K_{OW}$  is listed in Table 1. In solution-phase experiments, NAPH, PHEN, and PYR were used as  $\pi$ -donor compounds, and 1,2,4-trichlorobenzene (TCB, Aldrich) and TeCB were used as non- $\pi$ -donor controls.

Egg phospholipids were purchased from Lipoid (Ludwigshafen, Germany). Based on the information provided by the manufacturer, the lipids contain 97.1% phosphatidylcholine (structure shown in Figure S1, Supporting Information). Solution-phase carbon nuclear magnetic resonance (<sup>13</sup>C NMR) spectra of the phospholipids in chloroform were acquired on a Bruker-DRX 500 MHz spectrometer (Germany) (Figure S2, Supporting Information). Fourier-transform infrared (FTIR) spectra of the phospholipids and  $Cu^{2+}$ -complexed phospholipids with KBr Pellet were acquired on a Thermo Nexus 870 spectrometer (USA) (Figure S3, Supporting Information). In pH titration experiments, 0.05 M HCl was added continuously at 25  $\mu$ L each time (equivalent to 1.25 micromole) to 40 mL suspension of phospholipids (679 mg/L) in 0.02 M  $NaNO_3$  at 30 °C (Figure S4, Supporting Information).

**Batch Sorption.** Phospholipids were mixed with 0.02 M  $NaNO_3$  aqueous solution under continuous stir to prepare a homogeneous gel phase suspension containing 0.15–2.0 g/L phospholipids. Aqueous stock solution of  $Cu^{2+}$  (327 mg/L), if needed, was added directly to phospholipid suspension to give a concentration of 3 mg/L, followed by pH adjustment to about 6 by NaOH and HCl. For metal-free phospholipid suspension, the pH (~6) was unadjusted except where noted, which was adjusted by 0.05 M  $HNO_3$  and NaOH. Sorption experiments were carried out in 20 mL or 40 mL amber EPA vials equipped with Teflonlined screw caps. Vials received sufficient volume of phospholipid suspension, followed by sorbate in methanol carrier (TNB in acetonitrile) that was

kept below 0.1% by volume to minimize cosolvent effects. The amount of phospholipids and the volume of solution were selected for each sorbate to ensure data compatibility while maintaining analytical accuracy. Sorption isotherm of  $Cu^{2+}$  to phospholipids was obtained from separate experiments (Figure S5, Supporting Information). Duplicate samples were done for sorption isotherms, and four or five replicate samples for single-concentration sorption. The samples were shaken by an orbital shaker incubated at 20 ± 0.5 °C for 2 h. This period of time was sufficient to reach sorption equilibrium for organic solutes based on previous kinetic studies (data not shown). Afterward, the samples were centrifuged at 4000 rpm (1500g) for 30 min and then left undisturbed on a flat surface for more than 12 h to allow complete separation between gelled phospholipids and solution. The supernatant was clear in vision and showed negligible optical density (300 nm) compared to a value of 0.68 for the phospholipid suspension (0.217 g/L). The pH values measured at sorption equilibrium were very close (generally <0.2 pH units) between metal-free (5.9–6.3) and metal-containing samples.

Solute from an aliquot of the aqueous phase was analyzed directly by high-performance liquid chromatography (HPLC) using a 4.6 × 150 mm HC-C18 column (Agilent). Isocratic elution was performed with a UV detector under the following conditions: 80% methanol:20% water (v:v) with a wavelength of 254 nm for NAPH; 90% methanol:10% water with a wavelength of 254 nm for PHEN; 70% methanol:30% water with a wavelength of 262 nm for NBZ; 60% methanol:40% water with a wavelength of 238 nm for DNB; 55% methanol:45% water with a wavelength of 266 nm for TNB; 50% methanol:50% water with a wavelength of 270 nm for PHOL; 80% methanol:20% water with a wavelength of 231 nm for DCP; 75% methanol:25% water (v:v) with a wavelength of 210 nm for DNL; 80% methanol:20% water with a wavelength of 220 nm for DCB; 90% methanol:10% water with a wavelength of 220 nm for TeCB. Isocratic elution was performed with a fluorescence detector under the following conditions: 90% methanol:10% water with excitation/emission wavelengths of 355/402 nm for ANEN; 90% methanol:10% water with excitation/emission wavelengths of 334/391 nm for PYR. Metal concentration in the aliquot was measured by a Hitachi Z-8100 atomic absorption (AA) spectrometer (Japan). To take account for solute loss from processes other than sorption to phospholipids (i.e., metal adsorption to glassware, and organic sorption to septum and volatilization), calibration curves were obtained separately from controls receiving the same treatment as the sorption samples but no phospholipids. Calibration curves included at least seven standards over the tested concentration range. Based on the obtained calibration curves, the sorbed mass of organic solute

or heavy metal was calculated by subtracting the mass in the aqueous phase from the mass spiked.

Phospholipids in suspensions are expected to exist as mixtures of multilamellar liposomes and amorphous liposome coagulates. The average hydrodynamic diameter ( $D_H$ ) of the lipid aggregates in 0.02 M NaNO<sub>3</sub> solution at 25 °C was determined with a scattering angle of 0–135 degree using a laser particle size analyzer (Mastersizer 2000) (MALVERN, UK) (Figure S6, Supporting Information).  $D_H$  keeps nearly constant within the pH range of 4–8.5, but increases greatly from 0.54 to 6.8 μm when the phospholipids/solution ratio decreases from 2 to 0.09 g/L. A separate test on phenanthrene sorption showed that changing the phospholipids/solution ratio (0.11–0.83 g/L) did not affect the lipid–water partition coefficient ( $K_d$ ) (data not shown). We also compared sorption of 1,3-dinitrobenzene and phenanthrene between the phospholipid suspension by our method and that by a referenced method (17), which contains mainly small unilamellar vesicles of phospholipids. No differences in  $K_d$  were observed between the two suspensions (data not shown). Moreover, the phospholipids throughout the operation of batch sorption experiments should be chemically stable considering earlier results that solution-phase soya phospholipids exposed to atmosphere were resistant to oxidation within 8 days (18).

**Solubility Enhancement Experiments.** To test the hypothesis of cation- $\pi$  bonding between PAHs and Cu<sup>2+</sup> ions complexed to phospholipids, saturated solubility of anhydrous CuSO<sub>4</sub> (>99%) in chloroform was measured in mixtures of NAPH, PHEN, PYR, and TCB. Vials containing mixtures of CuSO<sub>4</sub> powder and organic solute in chloroform were covered with aluminum foil from light and shaken in an orbital shaker at 20 ± 1 °C for 7 d. After centrifugation, 3 mL of solution was withdrawn carefully by syringe and mixed with 3 mL of deionized water for Cu<sup>2+</sup> extraction. The concentration of Cu<sup>2+</sup> in the aqueous phase was measured by AA. The extraction efficiency of Cu<sup>2+</sup> from chloroform by water was tested to be 100%.

**Solution-Phase <sup>1</sup>H NMR Experiments.** Aqueous phospholipid suspension was adjusted to the desired pH (3.0, 3.5, 3.9, 4.7, 6.0) by 0.05 M HNO<sub>3</sub> and NaOH, followed by filtration through a 0.45 μm membrane. The obtained gel-phase phospholipids was freeze-dried and stored for later use in the NMR experiments. <sup>13</sup>C NMR spectra of the obtained phospholipids in chloroform (results not shown) were found identical to that of the untreated phospholipids (Figure S2, Supporting Information), suggesting no chemical variation during the course of treatment. Moreover, a separate test on phenanthrene sorption showed similar partition coefficients to the treated and the untreated phospholipids (data not shown). <sup>1</sup>H NMR spectra of mixtures of PHEN or TeCB and phospholipids in chloroform-*d* (99.8% D) were recorded at room temperature on a Bruker-DRX 500 MHz spectrometer. The spectrometer was locked on chloroform-*d* and chemical shifts ( $\delta$ ) were internally referenced to TMS. Moreover, <sup>1</sup>H NMR spectra of mixtures of triethylamine cation, used as a model compound for protonated amine groups of phospholipids, and NAPH, PHEN, PYR, or TCB in chloroform-*d* were also acquired.

## Results and Discussion

**Characterization of Phospholipids.** Elemental analysis on freeze-dried phospholipids gave: C (66.5), H (10.9%), N (1.9%), and S (<0.5%, below detection) on a weight basis. The phospholipids used in this study are phosphatidylcholine (97.1%), which is structured with a polar head composing a charged amine group and a phosphate group and two long chains of fatty acid residues (Figure S1, Supporting Information). <sup>13</sup>C NMR spectra of selected reference standards of different phospholipids have been summarized in literature (19). In this study chemical shifts (ppm) of solution-phase

<sup>13</sup>C NMR spectra from the phospholipids in chloroform verified regions of methyl/methylene (14.5–34.7), glycerol and polar headgroup (54.7–70.9), olefinic region (128.2–130.6), and carbonyl (173.5, 173.9) (Figure S2, Supporting Information). Figure S3 in Supporting Information displays the FTIR spectra of the phospholipids and Cu<sup>2+</sup>-complexed phospholipids. According to an earlier FTIR study of Lecithin (20), the bands between 3012 and 2852 cm<sup>-1</sup> are assigned to  $\nu_s$  and  $\nu_{as}$  of methyl/methylene, the band at 1737 cm<sup>-1</sup> to  $\nu$ (CO), the band at 1251 cm<sup>-1</sup> to  $\nu_{as}$ (PO<sub>4</sub><sup>-</sup>), the band at 1094 cm<sup>-1</sup> to CH<sub>2</sub> wag and CH<sub>2</sub> twist, and the band at 1468 cm<sup>-1</sup> to a combination of  $\nu_{as}$ (CN<sub>2</sub>),  $\delta_{as}$ (CH<sub>3</sub>), and CH<sub>2</sub> sciss. Note sorption of Cu<sup>2+</sup> to phospholipids changes  $\nu$ (CO) to 1739 cm<sup>-1</sup>, and  $\nu_{as}$ (PO<sub>4</sub><sup>-</sup>) to 1246 cm<sup>-1</sup>, implying Cu<sup>2+</sup> complexation to these functionalities.

**Batch Sorption.** Sorption isotherms plotted as sorbed concentration ( $q$ , mmol/kg) vs solution concentration ( $C_e$ , mmol/L) at sorption equilibrium are shown in Figure 1 for selected compounds. Sorption isotherms or single-concentration sorption data with presence of Cu<sup>2+</sup> for the same sorbates are shown together in Figure 1 for comparison. Phospholipid-water distribution coefficients with and without the presence of Cu<sup>2+</sup> ( $K_{d,Cu}$  and  $K_d$ , respectively) were calculated for all sorbates, and the average values from all sorption points (isotherm or single-concentration data) with standard deviations are listed in Table 1. Ratios of  $K_{d,Cu}$  to  $K_d$  were also calculated for all sorbates and shown in Table 1. Sorption isotherms of the selected compounds (PHEN, DNB, PHOL, see Figure 1) are highly linear ( $R^2$  between 0.97 and 0.99 in linear regression), indicating the predominant role of hydrophobic effects in sorption. Consistent with the mechanism of hydrophobic partition, a good linear free energy relationship was found between  $K_d$  and  $K_{OW}$  for the low-polar compounds (PAHs, chlorobenzenes, NBZ, DNL) (Figure 2). As expected the high-polar compounds (PHOL, DCP, DNB, TNB) are displaced upward by 0.30–0.91 units relative to the regression line from the low-polar compounds, suggesting additive polar (e.g., dipole–dipole) extra-interactions with the functional groups of phospholipids. Earlier studies have shown similar results that the partitioning of polar organic solutes is higher than predicted based on the log  $K_d$  vs log  $K_{OW}$  relationships from nonpolar solutes (2, 4).

A striking observation can be made is that the presence of Cu<sup>2+</sup> at a low level of 3 mg/L (initial concentration) increases sorption of the three and four-ring PAHs (PHEN, ANEN, and PYR) by 1.7–5.2 times (measured as ratio of  $K_{d,Cu}$  to  $K_d$ , see Table 1), while leaves sorption of the rest solutes nearly unchanged. The three and four-ring PAH molecules have highly delocalized  $\pi$ -electrons and may act as strong electron-donors when interacting with electron-deficient species such as cations. The enhanced PAH sorption by Cu<sup>2+</sup> was likely due to cation- $\pi$  interactions between PAHs and Cu<sup>2+</sup> ions complexed to phospholipid functional groups (amine, phosphate, carbonyl) (sorption isotherm of Cu<sup>2+</sup> shown in Figure S5, Supporting Information). Compared to the three and four-ring PAHs, the rest compounds tested in this study are weak  $\pi$ -donor (NAPH) or non- $\pi$ -donors (chlorobenzenes, NACs, phenolics, DNL), and therefore cannot invoke strong cation- $\pi$  interactions.

Cation- $\pi$  bonding between electron-rich aromatic structures and free or complexed metal ions (e.g., Cs<sup>+</sup>, Ag<sup>+</sup>, Cu<sup>+</sup>, Co(NH<sub>3</sub>)<sub>6</sub><sup>3+</sup>, Cu<sup>2+</sup>) toward molecular recognition and selective metal binding has been well documented in literature (21–29). For example, Ag<sup>+</sup> and Cs<sup>+</sup> were found to be selectively bound by calixarenes in aqueous solution via cation- $\pi$  interactions (21, 22). The cation- $\pi$  bonding between aromatic  $\pi$ -donors (thiophene, phenanthrene) and soft transition metal ions (Ag<sup>+</sup>, Cu<sup>+</sup>) complexed on the mineral surface was also proposed to account for the strong sorptive affinities of these chemicals (26, 27). The cation- $\pi$  bonding of complexed Cu<sup>2+</sup>

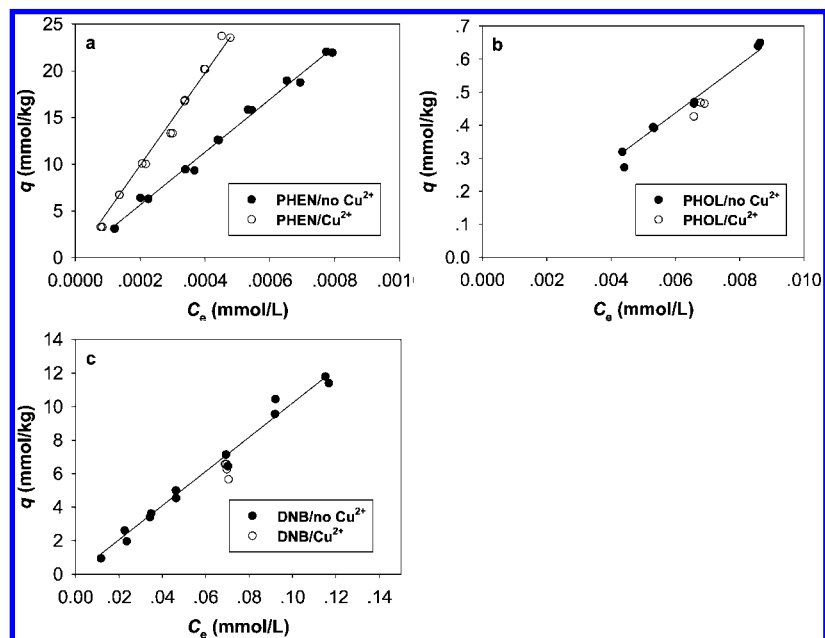


FIGURE 1. Isotherms or single-concentration data (four or five replicates) plotted as equilibrium sorbed concentration ( $q$ ) vs aqueous phase concentration ( $C_e$ ) with and without presence of  $\text{Cu}^{2+}$ . (a) PHEN. (b) PHOL. (c) DNB. Lines represent linear model fittings to sorption isotherms.

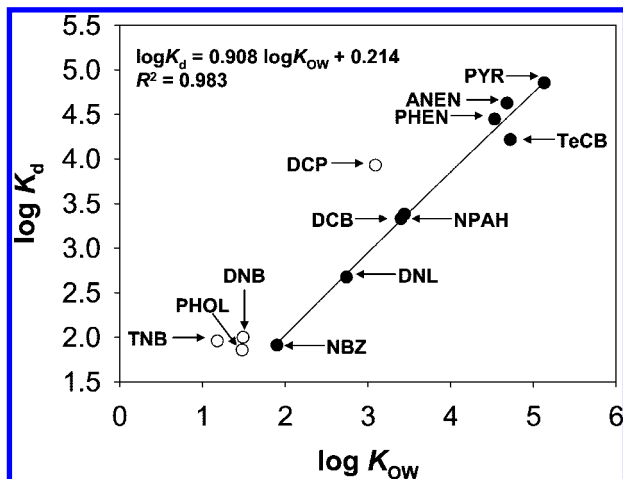


FIGURE 2. Phospholipid–water distribution coefficient ( $K_d$ ) vs  $n$ -octanol–water partition coefficient ( $K_{ow}$ ) for different solutes. The line and equation are from linear regression on low-polar compounds (PAHs, chlorobenzenes, NBZ, DNL) shown in solid circles. High-polar compounds (PHOL, DCP, DNB, TNB) are shown in empty circles.

with indole rings of neighbor tryptophan residues plays a key role in connection of the chains of (L-tryptophylglycinato)Cu(II), as well as the exchange interactions between  $\text{Cu}^{2+}$  and the chains (28, 29). It should be noted that in aqueous solution  $\text{Cu}^{2+}$  in fact causes “salting out” effect on PAHs, i.e., PAH solubility decreases with increasing  $\text{Cu}^{2+}$  concentration (30), suggesting no formation of  $\text{Cu}^{2+}$ -PAH complexes in aqueous solution. This is because the “desolvation penalty” induced by strong  $\text{Cu}^{2+}$  hydration is too high, and the cation- $\pi$  bonding between  $\text{Cu}^{2+}$  and PAHs is thus prohibited in aqueous solution. However, binding of  $\text{Cu}^{2+}$  to phospholipids is expected to create hydrophobic microenvironments surrounding the  $\text{Cu}^{2+}$  ion, relieving the “desolvation penalty” and thus facilitating cation- $\pi$  interactions. Previous studies indicated that cation binding to hydrophobic subunits of a water soluble host (macrocylic

polyethers, cryptands, cyclophanes) indeed greatly enhances the intensities of cation- $\pi$  interactions in aqueous solutions (23, 25).

Relationships of  $K_d$  vs pH from single-concentration experiments are shown in Figure 3 for sorption of selected compounds to phospholipids. For the three strong  $\pi$ -donors, PHEN, ANEN, and PYR,  $K_d$  increases respectively by 2.2, 3.2, and 4.2 times when pH decreases from  $\sim 7.2$  to  $\sim 5.2$ , but keeps relatively constant beyond this pH range. Alternatively, only small changes in  $K_d$  (generally  $< 20\%$ ) were observed for other tested compounds (NAPH, DNB, PHOL, and DCB) when pH decreases from  $\sim 7$  to  $\sim 4$ . Note within this pH range PHOL is dominated by the neutral form ( $pK_a$  of phenol is 9.89, ref 31), and other solutes are nonionic. Clearly, the pH effect on PAH sorption cannot be attributed to changes in hydrophilicity of functional groups due to the protonation/deprotonation transition because otherwise the same pH effect would have also been observed for other solutes. We propose that the enhanced sorption of three and four-ring PAHs at low pH was due to cation- $\pi$  interactions between PAHs (electron-donors) and the protonated amine groups (electron-acceptors) of phospholipids. Discovery of the cation- $\pi$  bonding between the ammonium subunit of acetylcholine and the aromatic tryptophan side chain (32) was considered a breakthrough in studying host-guest (e.g., protein-ligand) binding in biochemistry. Intensive research has been conducted thereafter on complexation of organic cations with synthetic receptors, including calixarenes and cyclophane (33–35). Decreases in pH make larger fractions of protonated amine groups that may act as electron-acceptors. Titration of phospholipids in aqueous suspension by HCl confirmed protonation of functional groups at pH between 4.6 and 7.1 (Figure S4, Supporting Information), which corresponds well to the pH range (5.2–7.2) for large changes in PAH sorption, providing extra support for the mechanism of cation- $\pi$  bonding. The rest compounds tested in pH studies are non- $\pi$ -donors (DNB, PHOL, and DCB) or weak  $\pi$ -donor (NAPH), and therefore did not show protonation facilitated sorption via cation- $\pi$  bonding.

We recently proposed cation- $\pi$  bonding with transition metal ions ( $\text{Ag}^+$ ,  $\text{Cu}^{2+}$ ,  $\text{Fe}^{3+}$ ) and charged amine groups on the bacterial surface, which is structured with multibiopoly-

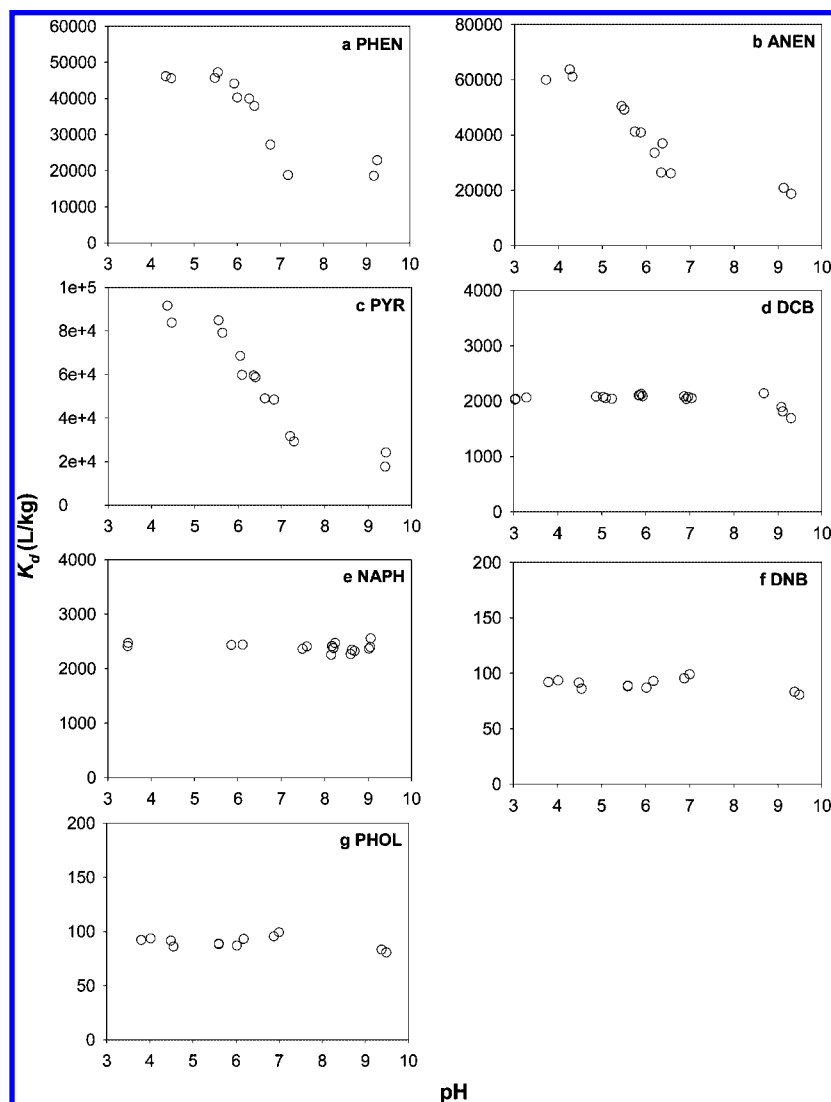


**FIGURE 3.** Phospholipid–water distribution coefficient ( $K_d$ ) vs pH at fixed initial concentrations (shown in parentheses) for different solutes. (a) PHEN (0.0049 mmol/L). (b) ANEN (0.0014 mmol/L). (c) PYR (0.0012 mmol/L). (d) DCB (0.033 mmol/L). (e) NAPH (0.028 mmol/L). (f) DNB (0.098 mmol/L). (g) PHOL (0.0076 mmol/L).

mers (e.g., polysaccharide, cross-linked shot peptides, lipoproteins, organic acids), responsible for the stronger facilitated sorption of phenanthrene (electron-donor) compared to tetrachlorobenzene (nonelectron-donor) (16). In this study, consistent effects by cobinding of proton and  $\text{Cu}^{2+}$  were observed on PAH sorption to a neat biopolymer of phospholipids. The observations further support the mechanism of cation- $\pi$  bonding in PAH sorption to the bacterial surface.

Considering the wide distribution of phospholipids and their derivatives in the environment, the PAH sorption facilitated by metal and proton binding to these biopolymers may have a profound impact on the environmental fate of PAHs. Furthermore, because phospholipids are major constituents of the cytoplasmic membrane, the results also imply that coexisting heavy metal ions may affect the transport of PAH molecules into the membrane and possibly the associated toxic effects. It is worth noting although the enhanced sorption observed in this study is only a factor of 2–5 times in  $K_d$ , translated to free energies of 1.7–3.9  $\text{kJ mol}^{-1}$ , it may heavily disturb the fine-tuned biological systems that have been in long-term evolution to take advantage of small thermodynamic gradients. For example, the potassium channel in cellular membranes can selectively extract  $\text{K}^+$  over  $\text{Na}^+$  at a ratio of 1000:1 from aqueous solution using the cation- $\pi$  bonding mechanism despite the small difference

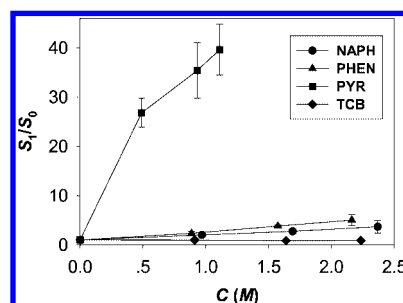


**FIGURE 4.** Ratio of saturated solubility of  $\text{CuSO}_4$  ( $S_1$ ) in mixtures of  $\pi$ -donors, NAPH, PHEN, and PYR, and non- $\pi$ -donor control, TCB, in chloroform to saturated solubility of  $\text{CuSO}_4$  in neat chloroform ( $S_0$ ,  $0.012 \pm 0.006$  mg/L) vs solute concentration ( $C$ ). Error bars, in some cases smaller than the symbols, represent standard deviations calculated from three replicates. Lines are for visual clarity only.

in binding energy (1.4 kcal/mol) between 1:1 complexes of  $\text{K}^+$ -benzene and  $\text{Na}^+$ -benzene (36).

**Solubility Enhancement Studies.** Figure 4 shows the saturated solubility of anhydrous  $\text{CuSO}_4$  vs concentration of NAPH, PHEN, PYR, and TCB in chloroform. Clearly, the presence of  $\pi$ -donor PAHs increases the solubility of  $\text{CuSO}_4$ ,

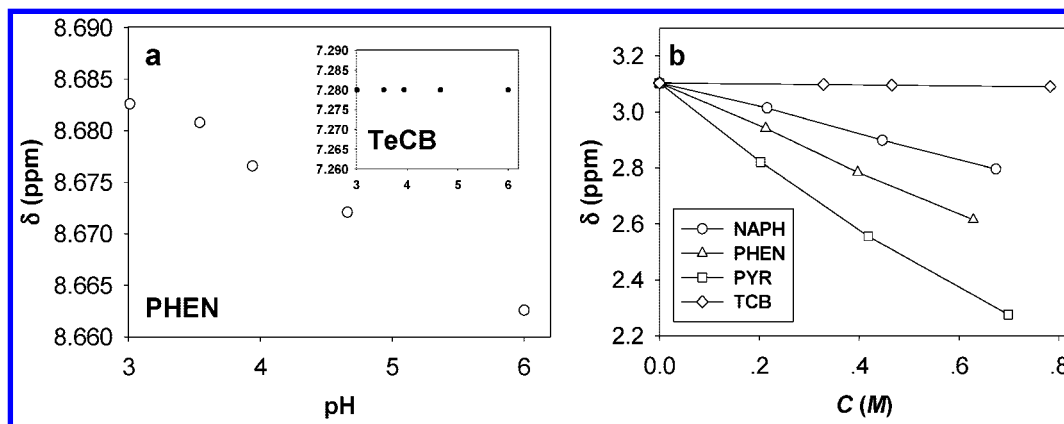


**FIGURE 5.**  $^1\text{H}$  NMR chemical shifts ( $\delta$ ) observed in chloroform-*d*. (a)  $\pi$ -Donor PHEN (0.005 M, 4,5 H) and non- $\pi$ -donor TeCB (0.005 M, 3,6 H) shown separately on same  $\delta$  scales (0.030 ppm) in mixtures of phospholipids (200 mg/mL) vs pH for phospholipid preparation. (b) Triethylamine cation (0.012 M,  $\text{N}^+\text{CH}_2^-$ ) in mixtures of  $\pi$ -donors, NAPH, PHEN, and PYR, and non- $\pi$ -donor control, TCB, vs solute concentration ( $C$ ). Lines are for visual clarity only.

and the solubility enhancement correlates with  $\pi$ -donor ability of PAH (PYR > PHEN > NAPH). NAPH, PHEN, and PYR increase the solubility up to  $4 \pm 1$  times (measured as ratio to saturated solubility in neat chloroform, with standard deviations calculated from three replicates),  $5 \pm 1$  times, and  $37 \pm 5$  times, respectively, with the examined concentrations. In contrast, the saturated solubility of  $\text{CuSO}_4$  in chloroform keeps nearly constant when the concentration of TCB, a non- $\pi$ -donor, increases to similar levels. The results strongly suggest that cation- $\pi$  complexes are formed between PAHs and  $\text{Cu}^{2+}$  in chloroform. In a media of organic solvent like chloroform, the cation-hydration induced “desolvation penalty” no longer exists, and therefore cation- $\pi$  bonding is thermodynamically favored. One can imagine that the hydrophobic aliphatic residues of phospholipids are somehow coiled to encompass the complexed metal ions, which facilitates cation- $\pi$  bonding of the metal ion in the aqueous phase by relieving the “desolvation penalty”.

**Solution-Phase  $^1\text{H}$  NMR Studies.** The electron coupling between protonated amine groups of phospholipids and PAHs is supported by observations in the solution-phase  $^1\text{H}$  NMR experiments. Placing a nucleus above or below the plane of an aromatic structure results in electronic shielding due to the “ring current” effect (37). Thus when cation- $\pi$  complexes are formed between ammonium cations and PAHs, upfield chemical shifts (shielding) of proton/carbon resonances would be expected for the cation, and correspondingly downfield chemical shifts (deshielding) for the PAH. In previous studies  $^1\text{H}$  NMR and  $^{13}\text{C}$  NMR upfield shifts of the phenyl and methyl groups of trimethylphenyl ammonium have been used to verify inclusion of the cation into the cavity of cone-shaped *p*-sulfonatocalix[4]arene in water (33). Compared to non- $\pi$ -donor TeCB, a clear trend of  $^1\text{H}$  NMR downfield shifts (up to 0.02 ppm) was observed for  $\pi$ -donor PHEN with increasing protonation of phospholipid functional groups as pH decreases from 6.0 to 3.0 (Figure 5a). The observation is best described by the acidification-enhanced cation- $\pi$  bonding between the protonated amine groups of phospholipids and PHEN.

To further verify cation- $\pi$  bonding between PAHs and the protonated amine groups of phospholipids, the  $^1\text{H}$  NMR spectrum was collected for a model compound, triethylamine cation in chloroform with presence of  $\pi$ -donor. High  $^1\text{H}$  NMR upfield shifts (shielding) of triethylamine cation (up to 0.24 ppm for  $\text{N}^+\text{H}$ , 0.83 ppm for  $\text{N}^+\text{CH}_2^-$ , and 0.62 ppm for  $-\text{CH}_3$ ) were observed in mixtures of NAPH, PHEN, and PYR, and the shifts also correlate with  $\pi$ -donor strength of PAH (PYR > PHEN > NAPH) (Figure 5b). Alternatively, negligible upfield shifts (0.01 ppm) were observed for TCB considered a non- $\pi$ -donor. These results indicate cation- $\pi$  bonding between

triethylamine cation and PAHs in chloroform. To be consistent with the  $^1\text{H}$  NMR results, we showed in earlier studies (16) that the aqueous solubility of phenanthrene ( $\pi$ -donor) is much more enhanced than pentachlorobenzene (non- $\pi$ -donor) by triethylamine cation, implying cation- $\pi$  bonding between the cation and phenanthrene in aqueous solution.

### Acknowledgments

This work was supported by the China National Science Foundation (grants 20637030 and 20777031) and Jiangsu Province Science Foundation (BK2006128). We thank Mr. Wei Zhu (Modern Analysis Center, Nanjing University) for assisting with the FTIR experiments.

### Supporting Information Available

Figures presenting chemical structure and  $^{13}\text{C}$  NMR and FTIR spectra of phospholipids, pH titration of phospholipids by HCl,  $\text{Cu}^{2+}$  sorption to phospholipids, and hydrodynamic diameter of phospholipid aggregates in aqueous suspension analyzed by laser scattering. This information is available free of charge via the Internet at <http://pubs.acs.org>.

### Literature Cited

- (1) Kelly, B. C.; Gobas, F. A. P. C.; McLachlan, M. S. Intestinal absorption and biomagnification of organic contaminants in fish, wildlife, and humans. *Environ. Toxicol. Chem.* **2004**, *23*, 2324–2336.
- (2) Barbato, F.; La Rotonda, M. I.; Quaglia, F. Chromatographic indexes on immobilized artificial membranes for local anesthetics: Relationships with activity data on closed sodium channels. *Pharm. Res.* **1997**, *14*, 1699–1705.
- (3) Go, M. L.; Ngiam, T. L. Thermodynamics of partitioning of the antimalarial drug mefloquine in phospholipid bilayers and bulk solvents. *Chem. Pharm. Bull.* **1997**, *45*, 2055–2060.
- (4) Osterberg, T.; Svensson, M.; Lundahl, P. Chromatographic retention of drug molecules on immobilised liposomes prepared from egg phospholipids and from chemically pure phospholipids. *Eur. J. Pharm. Sci.* **2001**, *12*, 427–439.
- (5) Lukacova, V.; Peng, M.; Tandlich, R.; Hinderliter, A.; Balaz, S. Partitioning of organic compounds in phases imitating the headgroup and core regions of phospholipid bilayers. *Langmuir* **2006**, *22*, 1869–1874.
- (6) Fox, C. B.; Horton, R. A.; Harris, J. M. Detection of drug-membrane interactions in individual phospholipid vesicles by confocal Raman microscopy. *Anal. Chem.* **2006**, *78*, 4918–4924.
- (7) Lazaro, E.; Rafols, C.; Abraham, M. H.; Roses, M. Chromatographic estimation of drug disposition properties by means of immobilized artificial membranes (IAM) and C18 columns. *J. Med. Chem.* **2006**, *49*, 4861–4870.
- (8) Ramos, J. L.; Duque, E.; Gallegos, M. T.; Godoy, P.; Ramos-Gonzalez, M. I.; Rojas, A.; Teran, W.; Segura, A. Mechanisms of solvent tolerance in gram-negative bacteria. *Annu. Rev. Microbiol.* **2002**, *56*, 743–768.

- (9) Tremblay, L.; Kohl, S. D.; Rice, J. A.; Gagné, J.-P. Effects of lipids on the sorption of hydrophobic organic compounds on geosorbents: A case study using phenanthrene. *Chemosphere* **2005**, *58*, 1609–1620.
- (10) Kohl, S. D.; Rice, J. A. Contribution of lipids to the nonlinear sorption of polycyclic aromatic hydrocarbons to soil organic matter. *Org. Geochem.* **1999**, *30*, 929–936.
- (11) Diné, H.; Schnitzer, M.; Mehuys, G. R. Soil lipids: Origin, nature, contents, decomposition and effect on soil physical properties. In *Soil Biochemistry*; Bollag, J. M., Stotzky, G., Eds.; Marcel Dekker: New York, 1990; Vol. 6, pp 397–429.
- (12) Bull, I. D.; van Bergen, P. F.; Nott, C. J.; Poulton, P. R.; Evershed, R. P. Organic geochemical studies of soils from the Rothamsted classical experiments-V. The fate of lipids in different long-term experiments. *Org. Geochem.* **2000**, *31*, 389–408.
- (13) Preston, C. M.; Shipitalo, S.-E.; Dudley, R. L.; Fyfe, C. A.; Mathur, S. P.; Lévesque, M. Comparison of <sup>13</sup>C-CPMAS NMR and chemical techniques for measuring the degree of decomposition in virgin and cultivated peat profiles. *Canadian J. Soil Sci.* **1987**, *67*, 187–198.
- (14) U.S. Department of Energy. *Chemical Contaminants on DOE Lands and Selection of Contaminant Mixtures for Subsurface Science Research*, U.S. DOE report no. DOE/ER-05471; U.S. Department of Energy: Washington, DC, 1992.
- (15) National Research Council. *Alternatives for Ground Water Cleanup*; National Academy Press: Washington, DC, 1994.
- (16) Xiao, L.; Qu, X.; Zhu, D. Biosorption of nonpolar hydrophobic organic compounds to *Escherichia coli* facilitated by metal and proton surface binding. *Environ. Sci. Technol.* **2007**, *41*, 2750–2755.
- (17) Escher, B. I.; Schwarzenbach, R. P. Partitioning of substituted phenols in liposome–water, biomembrane–water, and octanol–water systems. *Environ. Sci. Technol.* **1996**, *30*, 260–270.
- (18) Thompson, A. K.; Haisman, D.; Singh, H. Physical stability of liposomes prepared from milk fat globule membrane and soya phospholipids. *J. Agric. Food. Chem.* **2006**, *54*, 6390–6397.
- (19) Aursand, M.; Størseth, T. R.; Falch, E. Multi-component analysis of marine lipids in fish gonads with emphasis on phospholipids using high resolution NMR spectroscopy. *Chem. Phys. Lipids.* **2006**, *144*, 4–16.
- (20) Lever, V. T.; Ruggirello, A. FT-IR investigation of the urea state in Lecithin and sodium bis(2-ethylhexyl)phosphate reversed micelles. *J. Colloid Interface Sci.* **2003**, *258*, 123–129.
- (21) Bocchi, C.; Careri, M.; Casnati, A.; Mori, G. Selectivity of calix[4]arene crown-6 for cesium ion in ISE—effect of the conformation. *Anal. Chem.* **1995**, *67*, 4234–4238.
- (22) Ikeda, A.; Shinkais, S. Novel cavity design using calix[n]arene skeletons: Toward molecular recognition and metal binding. *Chem. Rev.* **1997**, *97*, 1713–1734.
- (23) Ma, J. C.; Dougherty, D. A. The cation- $\pi$  interaction. *Chem. Rev.* **1997**, *97*, 1303–1324.
- (24) Zaric, S. D. Cation- $\pi$  interaction with transition-metal complex as cation. *Chem. Phys. Lett.* **1999**, *311*, 77–80.
- (25) Gokel, G. W.; Barbour, L. J.; De Wall, S. L.; Meadows, E. S. Macrocyclic polyethers as probes to assess and understand alkali metal cation- $\pi$  interactions. *Coord. Chem. Rev.* **2001**, *222*, 127–154.
- (26) Yang, R. T.; Hernández-Maldonado, A. J.; Yang, F. H. Desulfurization of transportation fuels with zeolites under ambient conditions. *Science* **2003**, *301*, 79–81.
- (27) Zhu, D.; Herbert, B. E.; Schlautman, M. A.; Carraway, E. R.; Hur, J. Cation- $\pi$  bonding: A new perspective on the sorption of polycyclic aromatic hydrocarbons to mineral surfaces. *J. Environ. Qual.* **2004**, *33*, 1322–1330.
- (28) Costa, A. J.; Nascimento, O. R.; Ghivelder, L.; Calvo, R. Magnetic properties of carboxylate-bridged ferromagnetic copper(II) chains coupled by cation- $\pi$  interactions. *J. Phys. Chem. B.* **2001**, *105* (21), 5039–5047.
- (29) Nascimento, O. R.; Costa, A. J.; De Morais, D. I.; Ellena, J.; Delboni, L. F. Crystal structure and exchange pathways of the complex L-(tryptophyl-glycinato)copper(II). *Inorg. Chim. Acta* **2001**, *312* (1–2), 133–138.
- (30) Schlautman, M. A. Personal communication.
- (31) (Ed.) *Handbook of chemistry and physics*, 79th ed. Lide, D. R. Ed.; CRS Press: Boca Raton, FL, 1998.
- (32) Sussman, J. L.; Harel, M.; Frolow, F.; Oefner, C.; Goldman, A.; Toker, L.; Silman, I. Atomic structure of acetylcholinesterase from *Torpedo californica*: A prototypic acetylcholine-binding protein. *Science* **1991**, *253*, 872–879.
- (33) Shinkai, S.; Araki, K.; Matsuda, T.; Nishiyama, N.; Ikeda, H.; Takasu, I.; Iwamoto, M. NMR and crystallographic studies of a p-sulfonatocalix[4]arene-guest complex. *J. Am. Chem. Soc.* **1990**, *112*, 9053–9058.
- (34) Abraham, W. Inclusion of organic cations by calix[n]arenes. *J. Inclusion Phenom. Macrocyclic Chem.* **2002**, *43*, 159–174.
- (35) Wang, L.; Guo, D.; Chen, Y.; Liu, Y. Thermodynamics of interactions between organic ammonium ions and sulfonatocalixarenes. *Thermochim. Acta* **2006**, *443*, 132–135.
- (36) Kumpf, R. A.; Dougherty, D. A. A mechanism for ion selectivity in potassium channels: Computational studies of cation- $\pi$  interactions. *Science* **1993**, *261*, 1708–1710.
- (37) Jackman, L. M.; Sternhell, S. *Applications of Nuclear Magnetic Resonance Spectroscopy in Organic Chemistry*; 2nd ed.; Pergamon Press: Oxford, UK, 1969.
- (38) Schwarzenbach, R. P.; Gschwend, P. M.; Imboden, D. M. *Environmental Organic Chemistry*; 2nd Ed.; Wiley Interscience: NY, 2003.

ES0718117